Zeitschrift für Physikalische Chemie, Bd. 208, S. 225–238 (1999)
© by R. Oldenbourg Verlag, München 1999

Effect of the Microstructure of Copper Films on the Damping of Oscillating Quartz Resonators*

By M. Wünsche, H. Meyer, R. Schumacher

Atotech Deutschland GmbH, Erasmusstraße 20–24, 10553 Berlin

S. Wasle and K. Doblhofer

Fritz-Haber-Institut der Max Planck-Gesellschaft, Faradayweg 4–6, 14195 Berlin

(Received September 18, 1997; accepted December 1, 1997)

Quartz micro-balance / Damping resistance / Crystallinity / Impedance spectra / Electrical and mechanical properties of a quartz oscillator

An electrochemical procedure is described which allows the preparation of copper films of various crystallinity. Impedance spectra recorded for copper loaded quartz resonators were analysed in terms of the lumped-element circuit of the Butterworth-Van Dyke type to obtain their electrical and mechanical properties. Plots of the damping resistance versus film thickness indicate that the film's dissipation factor is significantly smaller in the case of disordered films with a finer crystallinity (10–100 nm) than in the case of more ordered structures having a grain size between 600–1500 nm. This observations states, that the finely structured copper phase behaves more rigid than the coarse material. The suggested explanation relates this effect to energy losses which occur during oscillation at the phase boundary of the grains by wearless internal friction. No contributions to the damping from surface roughness were observed for films thicker 0.5 μm. Thus, the damping of the quartz oscillator caused by different degrees of surface roughness of the generated copper films was of secondary importance, compared with the effect of the crystallinity.

1. Introduction

The application of oscillating quartz resonators operated in the shear mode to elucidate electrochemical and interfacial processes as well as the properties of the formed deposits has received considerable attention in the last

* Presented at the *5. Ulmer Elektrochemische Tage* on "Fundamental Aspects of Electrolytic Metal Deposition", June 23–24, 1997.

decade [1–6]. Theoretical aspects as well as experimental applications have been put forward and reviewed in various journals [7–10]. More recently, some experimentalists have focused their interest to the impedance of oscillating quartz resonators which they analysed in terms of the accepted electrical lumped-element circuit of the Butterworth-Van Dyke type [11–20]. This equivalent circuitry consists of a serial connection of ohmic, inductive, capacitive components and an additional parallel capacitance. By using modern impedance analyser systems the impedance measurement and the subsequently performed analysis allows a simultaneous determination of these individual electrical components within a few seconds. This type of measurement has been applied to various systems which includes polymer and metal layers deposited onto the quartz resonators [8, 9, 21].

In this study, the impedance measurement and the subsequently performed analysis were carried out on metallic copper deposits prepared electrochemically. They were investigated immediately after the electrochemical phase formation while the mass-loaded resonator still rested in the electrochemical environment. In addition, these measurements were also performed after the resonators had been removed from the electrochemical environment. All measurements were performed on copper layers of thickness up to 10 μm. This technique takes advantage of small elastic elongations of a few Angstroms which occur during the shear oscillation of the quartz resonator. This guarantees, that the electrical components, which are related to corresponding mechanical properties, are obtained under conditions which are strictly within the validity range of Hook's law.

In particular, the change of the ohmic resistance R_e for resonators operated in the shear mode is investigated for copper layers of varying thickness formed electrochemically on the quartz resonators. R_e is associated with the visco-elastic properties of the oscillating resonators, being a measure for energy dissipation E_d and damping [22]. It is shown, that these properties correspond to the relative acoustic impedance R_m^* of shear waves propagating to the finely and coarsely grained copper pahses deposited on the oscillating quartz resonators.

2. Experimental and evaluating procedures

2.1 Preparation of the quartz resonators and the electrolyte

Polished and roughened 5 MHz quartz crystals (AT-cut) supplied from KVG, Neckar-Bischofsheim were used as the resonators. The roughened blanks were prepared by applying a special chemical etch. The topographic pattern of a polished quartz blank (A) and polished and roughened platinized quartz blanks (B), (C), respectively, are shown in Fig. 1A–C. Note, that all experiments referred to later in the text were performed with gold coated resonators. They were prepared by evaporating a 100 nm thick

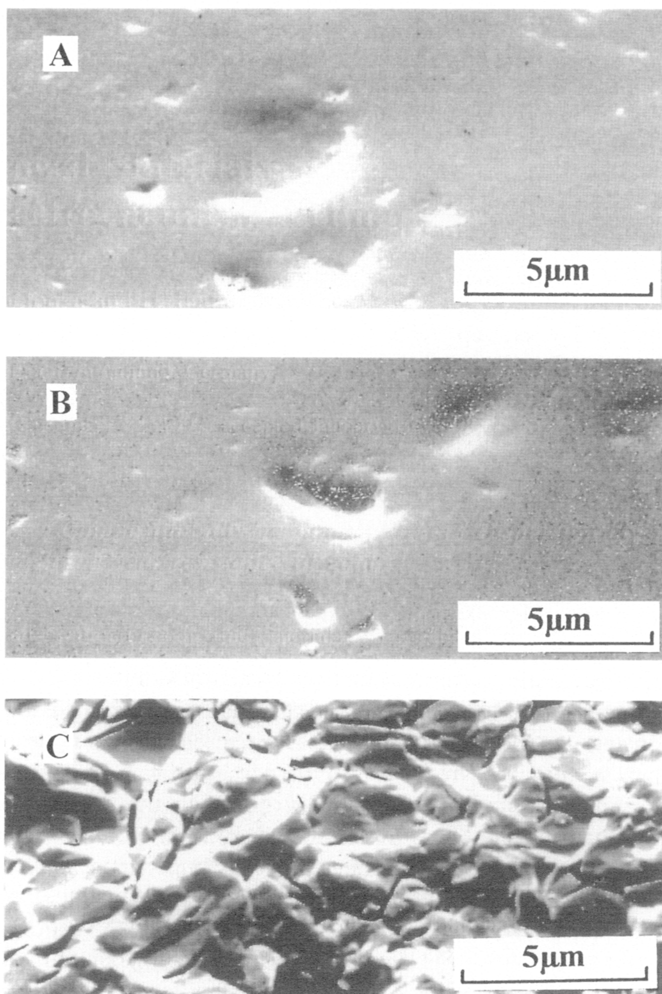

Fig. 1. Topographic pattern of 5 MHz quartz crystal oscillators (AT cut). A: polished quartz blank, B: platinized (100 nm) polished quartz blank, C: platinized (100 nm) roughened quartz blank.

circular Au layer (area: 0.5 cm^2) on both quartz faces. The resonators were mounted to a specially designed housing system which allows their fast and convenient replacement. The used electrolyte of the type H was made up from the following constituents: 0.3 mol $CuSO_4$, 2 mol H_2SO_4, 0.002 mol chlorid ions, 1 mg/liter $HO_3S\text{-}(CH_2)\text{-}S\text{-}S\text{-}(CH_2)_n\text{-}SO_3H$ with n between 2 and 4, 300 mg/liter $HO\text{-}(CH_2\text{-}CH_2\text{-}O\text{-})_{80}\text{-}H$. All potentials are given with respect to the saturated calomel electrode (SCE).

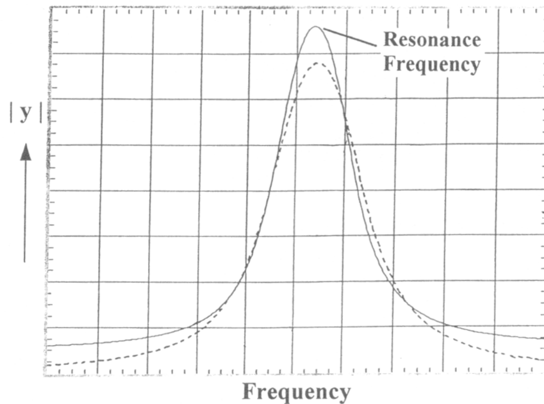

Fig. 2. Measured (solid line) and re-calculated (dashed line) impedance spectra of a copper loaded polished quartz resonator.

2.2 Experimental set-up and measuring procedure

Measurements in the immersed state

These experiments are performed in two consecutive steps. At first, a build up of a copper layer on top of the gold-coated quartz resonator is performed under a constant potentiostatic condition from an electrolyte H described in the previous section. The resulting frequency shift was measured with a frequency counter from Philips, type PM 6673. In the second step, at a certain mass load the sample is disconnected from the potentiostate (EG & G, type 273) and immediately connected to the Impedance Analyser from Hewlett Packard, type 4194A for recording the impedance spectrum of the mass loaded quartz resonators. During this measurement the sample is electrically disconnected from the electronic driver system but remains in the same electrolytic environment. A typical impedance spectrum recorded on a copper loaded resonator is represented in Fig. 2 as a solid line. To avoid sample modification which might be associated with the impedance measurement each sample is prepared by using a new quartz resonator freshly covered with a quantified mass load.

The film thickness and the volume of the deposit are calculated from the frequency shift of the quartz balance recorded during deposition by using the specific density of 8.96 g/cm^3 for bulk copper and the frequency-mass-calibration as given in Fig. 3. The quartz balance was calibrated by observing the frequency shift in the course of the electrochemical preparation of thick copper layers on top of polished gold coated resonators, and simultaneous weighing of these samples with a conventional lab microbalance.

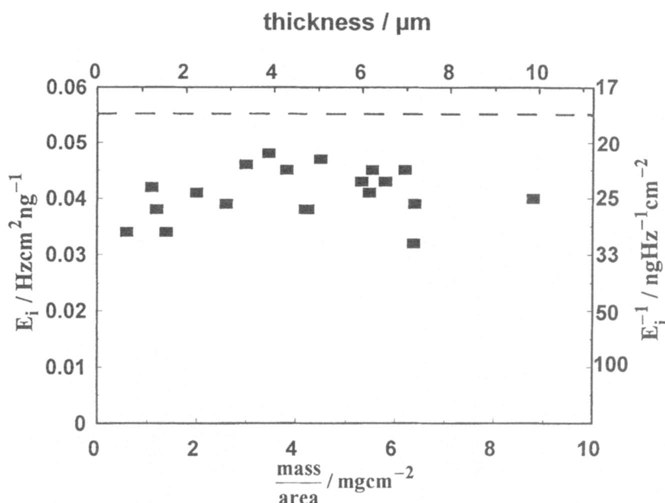

Fig. 3. Plot of the integral sensitivity E_i and its reciprocal E_i^{-1} vs. the copper mass load per unit surface area (lower abscissa) and film thickness (upper abscissa).

Measurements in the emersed state

After completing the measurement procedure in the immersed state some of the impedance measurements were repeated in the dry state after emersion of mass loaded resonator from the electrolyte. For these measurements the samples were cleaned from electrolytic residues by rinsing them with distilled water and finally with methanol. Subsequently, these samples were thoroughly dried with air. To exclude effects associated with liquids or electrolyte species trapped or adsorbed at the emersed sample, experiments were carried out on copper coated resonators prepared by evaporating technique under UHV conditions. It turned out that from this type of experiments and from those conducted after emersion no observations were obtained which might be associated with trapped liquids or adsorbed electrolyte species.

2.3 Data evaluation

The recorded impedance spectra (cf. Fig. 2) of the metallized quartz resonators were evaluated in terms of an electrical equivalent circuit of the Butterworth-van Dyke type [10, 12, 13]. This circuit consists of a serial connection of an ohmic resistance R_e, the inductive and capacitative elements L_e and R_e, respectively, and an additional parallel capacitance C_0. The subskript e denotes, that these components are elements of the electrical equivalent circuit developed for oscillating quartz resonators. R_e, L_e and C_e are called the motional arm for this electrical circuit. Their evaluation is

provided as an option of the Impedance Analyser which calculates R_e, L_e, C_e and C_0 from the recorded spectra. They describe the complete sample consisting of the quartz resonator plus the copper deposit. For measurements in the immersed state R_e is also affected by the electrolytic contact which causes an additional damping. As a result the R_e-value for a copper free resonator shifts to about 300 Ω compared to about 40 Ω obtained in the emersed state. As an example, the re-calculated spectrum (dotted line) obtained in the immersed state is given in Fig. 2 for comparison.

R_e and L_e are related to the resonator quality Q

$$Q = \omega L_e/R_e \tag{1}$$

with ω being the resonance frequency at a given mass load. R_e corresponds to the energy losses due to viscoelastic processes within the solid material. It is a measure for the damping of the acoustic wave propagating through the sample. The inverse of Q is directly proportional to the energy E_d dissipated in the resonator at a given ω

$$1/Q = \text{dissipated energy } E_d/\text{stored energy } E_s\,. \tag{2}$$

R_e is related to the acoustic impedance R_m (units: g/cm^2 s) of the corresponding mechanical equivalent circuit [10] through the relation

$$R_m = \omega M/Q\, A_{eff} k^2 \tag{3}$$

with M the actual mass load, A_{eff} the effective surface area and k^2 the square of the dimensionless electro-mechanical constant valid for a resonator which is not connected to an electronic driver device [10, 11, 23]. Since k^2 is expected to change significantly for resonators loaded with a considerable amount of mass, the relative acoustic impedance R_m^* which is proportional to $\omega M/QA_{eff}$ is used for data evaluation. Both R_m and R_m^* represent a material constant and should therefore be independent on the sample thickness.

3. Results

3.1 Preparation and characterization of copper films

Fine grained and coarsely structured copper films were prepared from the electrolyte H at −200 mV and −250 mV. Their cross section and topographic features (cf. Fig. 4A, B) were inspected with scanning electron microscopy (SEM). To avoid re-crystallization the SEM investigations conducted were recorded immediately after electrochemical film formation. Fig. 4A reveals, that at −200 mV a disordered finely grained material with a grain size distributed between 10 and 100 nm is obtained while, on the other hand, at −250 mV a more ordered coarsely structured copper material is formed with grains between 600 and 1500 nm in size [24, 25].

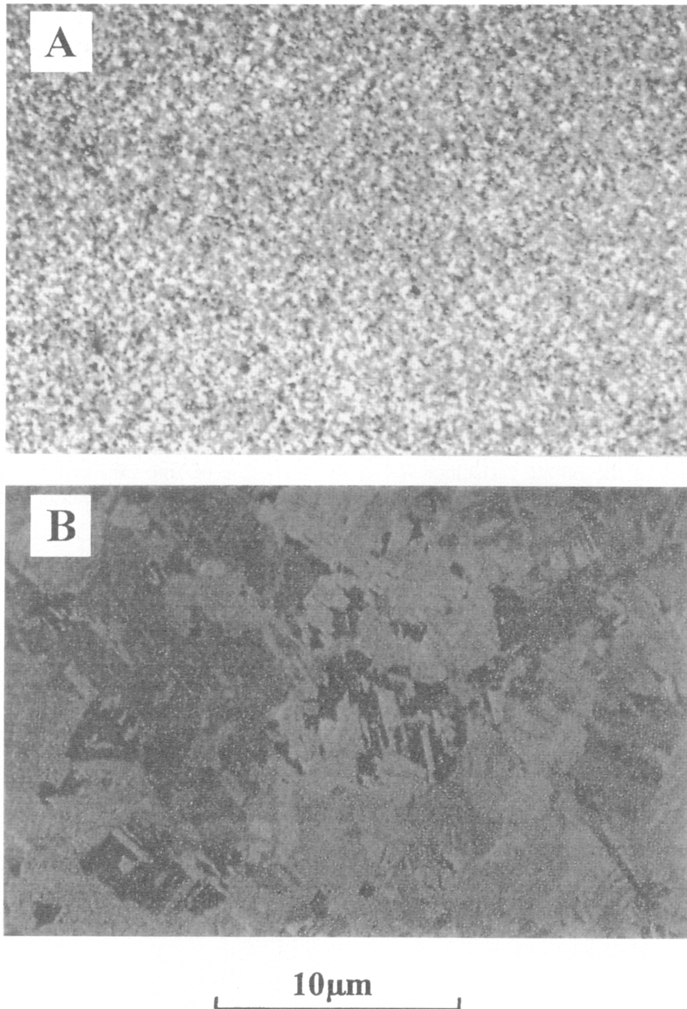

Fig. 4. Topographic features (REM) of copper deposits generated from electrolyte H at −200 mV (A) and −250 mV (B).

3.2 Damping and energy dissipation

Measurements in the immersed state

The change of the ohmic resistance R_e and the energy dissipation E_d are demonstrated in Figs. 5−6 for increasing copper mass loads deposited on polished quartz blanks. In these diagrams R_e or $1/Q$ are plotted versus the thickness of the copper deposits. The diagrams reveal slight changes for R_e

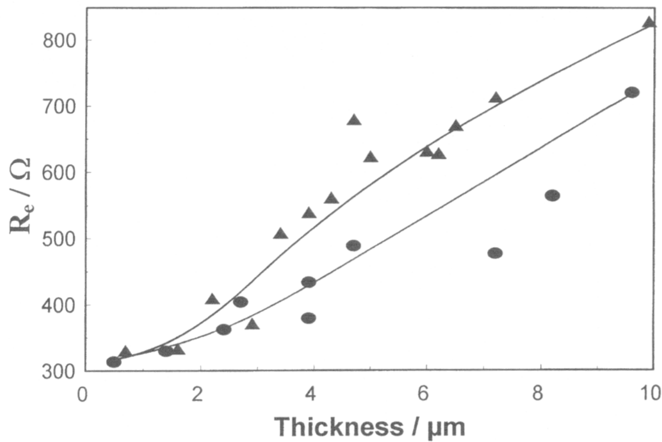

Fig. 5. Plot of the ohmic resistance R_e vs. the thickness of fine (●) and coarsely (▲) grained copper layers deposited onto polished resonators. The measurements refer to the immersed state.

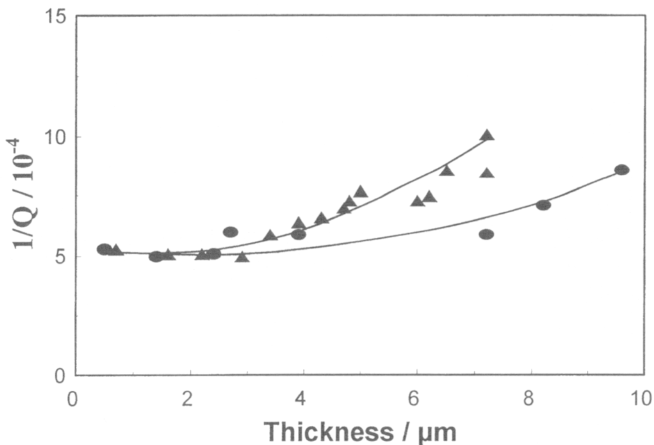

Fig. 6. Plot of the dissipated relative energy $1/Q$ vs. the thickness of fine (●) and coarsely (▲) grained copper layers deposited onto polished quartz resonators. The measurements refer to the immersed state.

and $1/Q$ for thin copper layers. However, for both R_e and $1/Q$ an increase with increasing mass load is observed. The curves obtained for the finely structured material run below those obtained for the coarse material.

The effect of surface roughness on R_e is described in Fig. 7. In this diagram R_e-values obtained on initially roughened (■) quartz blanks are

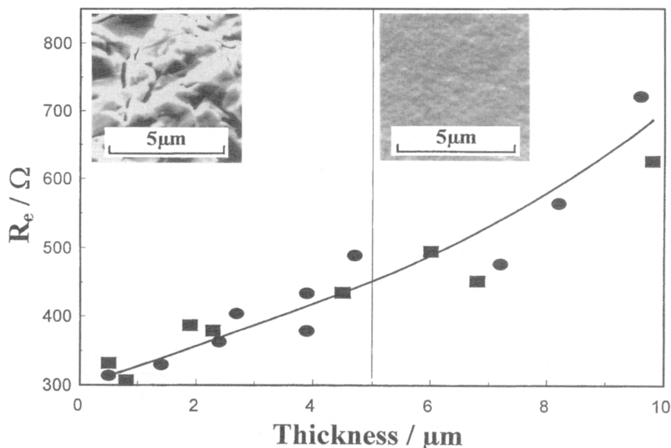

Fig. 7. Plot of the ohmic resistance R_e vs. thickness of fine (●) and coarsely (▲) grained copper layers deposited onto roughened resonators. The measurements refer to the immersed state. The insertions describe the change in surface roughness that occur during layer growth.

compared with those obtained by using polished (●) resonator blanks. The convincing match as presented in this diagram clearly demonstrates that a contribution of surface roughness to the overall damping is not detectable. The effect of roughness should be particularly clear for copper films below 5 μm. As shown in the inserts of Fig. 7 a major roughness change occurs in this range due to flattening of the initially roughened surface. This feature is generally observed for electrolytes as used here. However, the results of Fig. 7 suggest that damping associated with surface roughness becomes effective for films considerably thinner than 0.5 μm.

Measurements in the emersed state

The results of these investigations are shown in Fig. 8 as a plot R_e vs. thickness of the copper deposits. As expected, the R_e-values of samples without copper coating are considerably lower (40 Ω) compared to the immersed case (300 Ω). This change demonstrates the influence of the electrolyte contact to the overall damping of the resonator. The figure also reveals, that the course of the curves is directly comparable to those observed in experiments performed in the immersed state (cf. Fig. 5). However, the difference between R_e-values obtained for fine and coarsely structured material are much more pronounced in the emersed state.

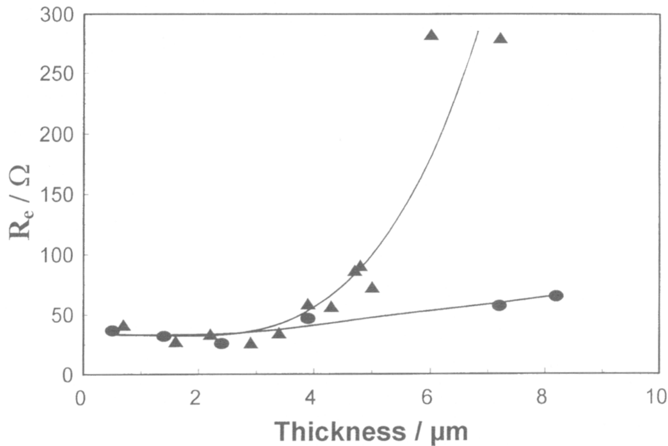

Fig. 8. Plot of the ohmic resistance R_e vs. the thickness of fine (●) and coarsly (▲) grained copper layers deposited onto polished quartz resonators. The measurements refer to the emersed state.

4. Discussion

4.1 Formal classification

The electrochemical formation and classification of differently structured copper phases has been subject to numerous studies which are extensively reviewed elsewhere [26, 27]. Fine and coarsely structured copper materials generated in this study were prepared from an acid copper electrolyte of the type H. The observation that these structure types were obtained from the same electrolyte by slightly changing the deposition potential from −200 mV to −250 mV suggests complicated formation kinetics associated with the continuous reproduction of the copper surface during vertical growth and the electrosorption kinetics of surface active additives. This was convincingly demonstrated by simultaneous *in situ* monitoring of charge and mass changes as well as changes of the surface reflectivity that occur during vertical film growth [24, 25]. The growth process of 3D metallic deposits has been related to continuous or discontinuous processes. The latter is dominated by nucleation phenomena forming macrosteps while the continuous type involves screw dislocations which later on form spirals and macrosteps [26, 27].

The obtained finely grained material is formally attributed to the randomly-oriented dispersion type, while the coarse material is ascribed to a field orientated texture type. The observed features are similar to those obtained on samples generated by varying the additive concentration as reported elsewhere [28]. In this study a mean grain size of about 35 nm was

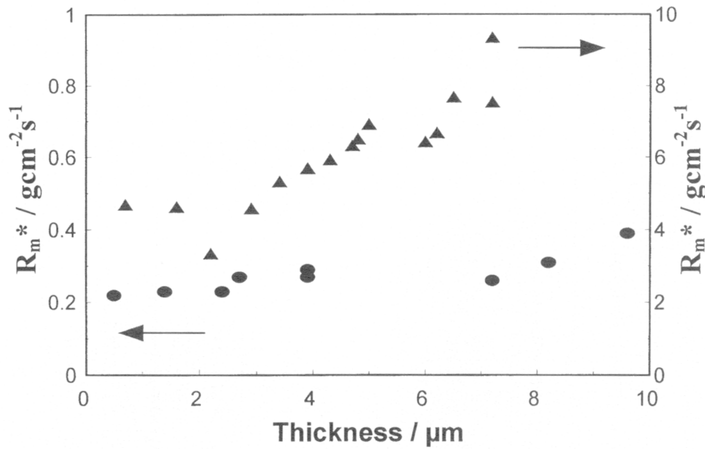

Fig. 9. Plot of the relative acoustic impedance R_m* vs. the thickness of fine (●) and coarsly (▲) structured copper layers. The measurements were taken on polished resonators and refer to the immersed state.

obtained for the dispersed phase while for the coarse structure a mean grain size of ca. 600 nm was reported. The dislocation density N_v for the finely structure phase yields 21×10^{10} cm^2 while the one for the coarse material has a smaller value of $N_v = 8 \times 10^{10}$ cm^2. The result, that the randomly-dispersed phase re-crystallizes almost completely upon thermal treatment while the coarsely grained material re-crystallizes incompletely (ca. 20%) is also consistant with observations obtained for materials generated in this work. Thus, the finely structured phase has to be considered as less ordered compared to coarsely grained material. Both structures are compact and pore-free.

4.2 Experimental results

It has been clearly stated in the Figs. 5−8, that differently structured copper films deposited on top of quartz resonators give rise to a different damping of the shear oscillations. The damping for the coarsely structured copper phase formed at −250 mV is larger than for the fine material generated at −200 mV. In agreement to this it was observed that the energy E_d dissipated in the copper coated resonators is also larger for the coarse material. As a consequence, the finely structured phase has a more rigid performance compared to the coarse material. This reflects that acoustic shear waves propagating through the coarse copper phase experience a larger energy dissipation compared to the finely structured copper phase.

The suggested explanation relates this observation to wearless internal friction that occurs at the phase boundary or in the bulk of the formed grains

[29−31]. The former situation assumes energy dissipation at the interface between the grains. In the latter case energy dissipation occurs in the bulk by movement of dislocations. However, this process can be disregarded since E_d is much larger for the coarsely grained material which in fact has a low dislocation density N_v. On the other hand, a small E_d is found for the finely structured phase having in fact a large N_v. This explanation is consistent with an atomistic model recently proposed to explain energy dissipation associated with the friction of sliding interfaces [29, 30]. This model takes into account, that energy dissipation that occur at sliding interfaces is associated with the geometry of the surface area of the sliding layers. E_d is expected to decrease for grains with a small surface area. This conclusion is based on the idea, that friction of two sliding interfaces leads to phonon excitation of surface sites which subsequently dissipates to acoustic and thermal energies.

The explanation, that wearless internal friction which might occur at the interface between the grains accounts for the observed energy dissipation is supported by the following approach in which R_e is transformed into the relative acoustic impedance R_m^* · R_m^* is a material constant and is expected to be independent of the film thickness but inversely related to the internal effective surface area A_{eff} between the grains. Assuming, that the grains have a cube-shaped geometry A_{eff} is related to the mean grain size å. R_m^* is re-calculated by using å = 50 nm for the finely grained material and å = 1000 nm for the coarse phase and presented in Fig. 9 as function of the thickness of the deposits. This evaluation refers to measurements performed while the resonator is exposed to the electrolytic solution. The observed increase in R_m^* of about 40% for both materials is most probably associated with the accuracy of the impedance analysis of the registered spectra. It has to be considered that the used electrical circuit changes for heavily loaded resonators. The results in Fig. 9 clearly reveal, however, that for this experimental situation R_m^* is much larger (about factor of twenty) for the coarsely grained material with respect to the fine structured phase. This evaluation is based on the assumption that a distinct phase boundary exists between the grains for both materials. This, however, is not necessarily the case for the finely structured dispersed material. As discussed earlier, the phase boundary between these grains is not well defined for either situation. In this case the estimated internal surface area A_{eff} has to be regarded as overestimated. As a result, the calculated R_m^*-values for small grains are probably slightly underestimated compared to the coarse grains.

Conclusion

In conclusion, the reported results obtained in the immersed and emersed state are consistent with the idea, that the propagating acoustic wave experi-

ences a larger damping for resonators coated with the more ordered coarsely structured material than for those coated with the disordered finely grained phase. Thus, the finely grained material has to be considered as more rigid compared to the coarsely structured phase. The suggested explanation relates this effect to energy losses which occur during oscillation at the phase boundary of the grains by wearless internal friction. It was further stated, that surface roughness does not contribute significantly to the damping for films thicker 0.5 μm.

References

1. J. H. Kaufmann, K. Kanazawa and G. B. Street, Phys. Rev. Lett. **53** (1984) 2461.
2. K. Kanazawa and J. Gordon, Anal. Chem. **57** (1985) 1771.
3. R. Schumacher, J. Pesek and O. Melroy, J. Chem. Phys. **89** (1985) 4338.
4. R. Schumacher, G. Borges and K. Kanazawa, Surf. Sci. **163** (1985) L621.
5. S. Bruckenstein and S. Swathirajan, Electrochim. Acta **30** (1985) 851.
6. S. Bruckenstein and M. Shay, Electrochim. Acta **30** (1985) 1295.
7. M. D. Ward and D. A. Buttry, Science **249** (1990) 1000.
8. R. Schumacher, Angew. Chem. **102** (1990) 347.
9. D. A. Buttry, in *Electroanalytical Chemistry. A Series of Advances*; Ed.: A. J. Bard, Marcel Dekker, New York (1991), Vol. 17, page 1–85.
10. D. A. Buttry and M. D. Ward, Chem. Rev. **92** (1992) 1355.
11. H. Muramatsu, E. Tamiya and I. Karube, Anal. Chem. **60** (1988) 2142.
12. K. S. Van Dyke, Proc. Annu. Freq. Control Symp. **10** (1956) 1.
13. K. S. Van Dyke, Phys. Rev. **25** (1925) 895.
14. C. Fruböse, K. Doblhofer and D. M. Soares, Ber. Bunsenges. Phys. Chem. **97** (1993) 475.
15. D. M. Soares, W. Kautek, C. Fruböse and K. Doblhofer, Ber. Bunsenges. Phys. Chem. **98** (1994) 219.
16. U. Pittermann, R. Reining and K. G. Weil, J. Electrochem. Soc. **141** (1994) 3416.
17. N. Yamamoto, T. Yamane, T. Tatsuma and N. Oyama, Bull. Chem. Soc. **68** (1995) 1641.
18. E. T. Watts, J. Krim and A. Widom, Physical Rev. **B 41** (1990) 3466.
19. J. Krim and A. Widom, Physical Rev. **B 38** (1988) 12184.
20. H. L. Bandey, M. Gonsalves, A. R. Hillman, A. Glidl and S. Bruckenstein, J. Electroanal. Chem. **410** (1996) 219.
21. D. Johannsmann, K. Mathauer, G. Wegner and W. Knoll, Phys. Rev. **B 46** (1992) 7808.
22. C. Lu (Editor): *Applications of Piezoelectric Quartz Microbalances*, Vol. 7, Elsevier, Amsterdam (1984).
23. H. Kuttruff, *Physik und Technik des Ultraschalls*, S. Hirzel Verlag, Stuttgart (1988).
24. M. Wünsche, H. Meyer and R. Schumacher, Circuit World **22** (1996) 4.
25. M. Wünsche, H. Meyer and R. Schumacher, Metalloberfläche **8** (1995) 578.
26. H. Fischer, *Elektrolytische Abscheidung und Elektrokristallisation von Metallen*, Springer Verlag, Berlin (1954).
27. E. Budevski, G. Staikov and W. J. Lorenz, *Electrochemical Phase Formation*, VCH Weinheim (1996).

28. I. Handreg, P. Klimanek and G. Lange, *Jahrbuch Oberflächentechnik Bd. 52*, Hüthig Verlag, Heidelberg (1996) S. 283.
29. G. M. McClelland, S. R. Cohen, in *Springer Series Surface Science* **22** (1990) 419.
30. G. M. McClelland, J. M. Glosli, in *Fundamentals of Friction: Macroscopic and Microscopic Processes,* NATO ASI Series **220** (1992) 405.
31. J. Krim, in *Spektrum der Wissenschaft* **12** (1996) 80.